Polym. Bull. (2014) 71:1–18
DOI 10.1007/s00289-013-1041-x

ORIGINAL PAPER

Synthesis and self-assembly of a new amphiphilic thermosensitive poly(*N*-vinylcaprolactam)/poly(ε-caprolactone) block copolymer

Qiuhua Wu · Liping Wang · Xiaofei Fu · Ximing Song · Qi Yang · Guolin Zhang

Received: 29 December 2012 / Revised: 1 June 2013 / Accepted: 21 August 2013 /
Published online: 31 August 2013

Abstract New amphiphilic thermosensitive poly(*N*-vinylcaprolactam)/poly(ε-caprolactone) (PNVCL-*b*-PCL) block copolymers were synthesized by ring-opening polymerization of ε-caprolactone with hydroxy-terminated poly(*N*-vinylcaprolactam) (PNVCL-OH) as a macroinitiator. The structures of the polymers were confirmed by IR, ^{1}H NMR and GPC. The critical micelle concentrations of copolymer in aqueous solution measured by the fluorescence probe technique reduced with the increasing of the proportion of hydrophobic parts, so did the diameter and distribution of the micelles determined by dynamic light scattering. The shape observed by transmission electron microscopy (TEM) demonstrated that the micelles are spherical. On the other hand, the UV–vis measurement showed that polymers exhibit a reproducible temperature-responsive behavior with a lower critical solution temperature (LCST). The LCST of PNVCL-OH can be adjusted by controlling the molecular weights, and that of copolymers can be adjusted by controlling the compositions and the concentration. Variable temperature TEM measurements demonstrated that LCST transition was the result of transition of individual micelles to larger aggregates.

Keywords Amphiphilic thermosensitive block copolymers · Ring-opening polymerization (ROP) · Self-assembly · Micelles · Lower critical solution temperature (LCST)

Q. Wu · L. Wang · X. Fu · X. Song · Q. Yang · G. Zhang (✉)
Liaoning Province Key Laboratory for Green Synthesis and Preparative Chemistry of Advanced Materials, College of Chemistry, Liaoning University, Shenyang 110036, People's Republic of China
e-mail: glzhang@lnu.edu.cn

Abbreviations

PNVCL-*b*-PCL	Poly(*N*-vinylcaprolactam)/poly(ε-caprolactone)
ε-CL	ε-Caprolactone
PNVCL-OH	Hydroxy-terminated poly(*N*-vinylcaprolactam)
ROP	Ring-opening polymerization
LCST	Lower critical solution temperature
PNVCL	Poly(*N*-vinylcaprolactam)
NVCL	*N*-vinylcaprolactam
$Sn(Oct)_2$	Stannous octoate
$HSCH_2CH_2OH$	2-Mercaptoethanol
AIBN	Azobisisobutyronitrile
THF	Tetrahydrofuran
CH_2Cl_2	Dichloromethane

Introduction

Polymeric micelles, self-assembled from amphiphilic block copolymers in selective solvents, are of intensive interest in contemporary macromolecular science for both their diversiform morphologies and potential applications [1–3]. The so-obtained macromolecular assemblies demonstrate a series of attractive properties in drug delivery systems, such as good biocompatibility and high stability in vitro and in vivo, and have been described as promising materials in applications such as biosensors, tissue engineering, and selective drug delivery [4–6].

Micelles formed by stimuli-responsive block copolymers have received much attention in recent years [7–9]. Stimuli-responsive polymers that exhibit unique property changes in response to environmental stimuli, for example, temperature, pH, electric fields, and light, are promising for many biomedical applications, including smart drug/gene delivery systems, injectable tissue engineering scaffolds, cell culture, and separation sheets [10–12]. Among all intelligent polymers studied temperature-responsive polymeric systems have drawn more attention, because this is the important physiological factor in the body, and some disease states manifest themselves by a change in temperature [13, 14]. Thermo-responsive polymers are soluble in cold water, though precipitate with heating above a certain temperature, known as the lower critical solution temperature (LCST) [15]. This phenomenon is reversible; upon cooling the thermosensitive polymers become soluble again [16].

Poly(*N*-vinylcaprolactam) (PNVCL) is a well-known thermosensitive polymer with a LCST near body temperature, approximately at 32 °C [17–19]. These physiological temperatures open perspectives for biomedical applications such as micro-encapsulation of enzymes or cells and drug delivery systems [20–22]. PNVCL can be used as a hydrophilic shell segment at temperatures below its LCST together with various kinds of hydrophobic moieties to make core/shell micelles. The actual interest in PNVCL is connected with the combination of its thermo-responsive properties, complexation ability with different therapeutic agents and biocompatibility [23, 24].

Poly(ε-caprolactone) (PCL) and their copolymers have attracted increasing attention in the pharmaceutical and medical fields for potential uses as bioresorbable sutures, orthopedic fixation devices, artificial skin, tissue engineering scaffolds, and drug delivery systems because their biodegradation in physiological conditions yields nontoxic products that can be bioabsorbed or excreted by the human body [25–28]. But the application of PCL for drug delivery has a drawback of slow degradation rate in vivo due to its high crystallinity and hydrophobicity [29–31]. Introduction of hydrophilic units has been used to improve biodegradability and hydrophilicity [32].

In this study, new amphiphilic thermosensitive poly(*N*-vinylcaprolactam)/poly(ε-caprolactone) (PNVCL-*b*-PCL) block copolymers were synthesized by ring-opening polymerization of ε-caprolactone (ε-CL) using hydroxy-terminated poly(*N*-vinylcaprolactam) (PNVCL-OH) as macroinitiator. Their structures were characterized. Then, the PNVCL-*b*-PCL micelles were prepared by solvent evaporation method and their physicochemical characteristics and thermosensitivities were investigated.

Experimental

Materials

N-vinylcaprolactam (NVCL, analytical grade) was purchased from Sigma-Aldrich and recrystallized from dry *n*-hexane prior to use. ε-Caprolactone (ε-CL) was purchased from Alfa Aesar Co., Ltd. Stannous octoate ($Sn(Oct)_2$) was purchased from Sigma-Aldrich Chemical Reagent Co., Ltd. 2-Mercaptoethanol ($HSCH_2CH_2OH$, analytical grade) was purchased from Amresco Co., Ltd. Pyrene was purchased from Alfa Aesar Co., Ltd. and recrystallized from dry ethanol prior to use. Azobisisobutyronitrile (AIBN, analytical grade) was purchased from Sinopharm Chemical Reagent Co., Ltd. (Shanghai, China), and recrystallized from dry ethanol prior to use. 1,4-Dioxane (analytical grade) and dichloromethane (CH_2Cl_2, analytical grade) were purchased from Sinopharm Chemical Reagent Co., Ltd. (Shanghai, China), dried and distilled prior to use. Other chemicals are all analytical reagents made in China and used without further purification.

Synthesis of hydroxy-terminated poly(*N*-vinylcaprolactam) (PNVCL-OH) (Scheme 1)

The PNVCL-OH was synthesized by the radical polymerization of NVCL monomer initiated by AIBN with $HSCH_2CH_2OH$ as chain transfer agents. In brief, 5.0425 g (0.0363 mol) of NVCL and 0.0597 g (0.3640 mmol) of AIBN were dissolved in 40 mL 1,4-dioxane and bubbling nitrogen for 30 min. Then, 0.0947 g (1.2141 mmol) of $HSCH_2CH_2OH$ was added into the reactor. The polymerization was performed at 68 °C and terminated after 24 h under stirring. After being cooled to room temperature, 1,4-dioxane was removed under reduced pressure. The resulting polymer was dissolved in 30 mL anhydrous CH_2Cl_2 and precipitated in 300 mL petroleum ether three times. The precipitate was dried under reduced pressure at 40 °C for 48 h giving the PNVCL-OH as white solid, yield 48 %.

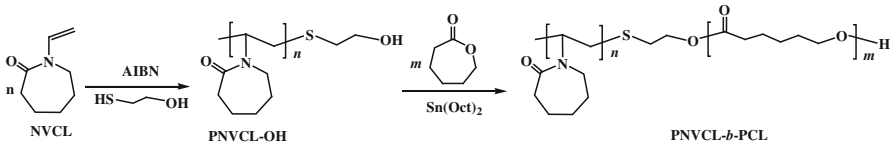

Scheme 1 The synthesis of PNVCL-*b*-PCL block copolymer

Synthesis of poly(*N*-vinylcaprolactam)/poly(ε-caprolactone) (PNVCL-*b*-PCL) block copolymer (Scheme 1)

The PNVCL-*b*-PCL block copolymers were synthesized by ring-opening polymerization of ε-CL initiated by PNVCL-OH with $Sn(Oct)_2$ as a catalyst. The necessary amounts of PNVCL-OH, ε-CL, $Sn(Oct)_2$ and toluene were added to a 50-mL round flask and after several cycles of evacuation-purging with purified nitrogen, the polymerization was performed in an oil bath at 120 °C and terminated after 48 h under stirring. After being cooled to room temperature and removal of toluene under reduced pressure, the resulting polymer was dissolved in 15 mL anhydrous CH_2Cl_2 and precipitated in 150 mL ethyl ether several times. The precipitate was dried in vacuum at 30 °C for 48 h to give the desired PNVCL-*b*-PCL block copolymers as white solid. The yield was approximately 30 %. Different molar ratios of the feeding ε-CL to PNVCL-OH resulted in the corresponding copolymers with various compositions as listed in Table 1.

Preparation of micelles

The micelles were prepared applying a solvent displacement method with a tetrahydrofuran/water (THF/H_2O) system [33]. A copolymer (50 mg) was first dissolved in 2.5 mL of THF; thereafter, the copolymer solution was slowly added into 10 mL of ultrapurified water (Aquaplus 18.2 MΩ). The THF was removed using a rotary evaporator at 25 °C for 2 h. The obtained solution was transferred into a 25-mL volumetric flask, followed by dilution to the calibration mark with ultrapurified water to obtain 2 mg mL^{-1} micelles.

Table 1 Related data on polymers

Sample	PNVCL-OH/ε-CL[a]	W_{PNVCL}/W_{PCL}^{b}	M_n^{b}	M_n^{c}	M_w/M_n	CMC (mg/mL)	Size (nm)[d]
PNVCL-OH	–	–	3,691	5,025	1.25	–	–
PNVCL-*b*-PCL**1**	1/10	84/16	4,375	7,417	1.12	2.7×10^{-2}	106
PNVCL-*b*-PCL**2**	1/20	70/30	5,287	8,230	1.09	5.2×10^{-3}	142
PNVCL-*b*-PCL**3**	1/30	52/48	7,111	9,217	1.05	3.1×10^{-3}	167

[a] Molar ratio of PNVCL-OH to ε-CL in feed

[b] Determined by ^1H NMR in $CDCl_3$ solution

[c] Determined by GPC in THF at 30 °C

[d] Determined by dynamic light scattering in aqueous solution at 25 °C

Characterization

The IR spectra were collected by a Perkin-Elmer FT-IR spectrometer using KBr disks. ^{1}H NMR spectra were measured on a Varian Mercury-300 NMR spectrometer at room temperature, using $CDCl_3$ as solvent. Chemical shifts (δ) were given in ppm using tetramethylsilane (TMS) as an internal reference. The gel permeation chromatography (GPC) measurement was conducted with a Waters 1515 GPC instrument equipped with a HT4 and HT3 column (effective molecular-weight range 5,000–600,000 and 500–30,000) and a 2414 differential refractive index detector. THF was used as eluent at the flow rate of 1.0 mL/min at 30 °C, and the molecular weights were calibrated with polystyrene standards. The lower critical solution temperature (LCST) of the aqueous solutions of the polymers was investigated on a Perkin-Elmer Lambda Bio 20 UV–vis spectrophotometer together with a NESLAB RTE-111 temperature controller. In brief, the polymers were dispersed in ultrapurified water (Aquaplus 18.2 MΩ). The transmittance of aqueous solutions of polymer at $\lambda = 500$ nm was recorded in a 1.0-cm path-length quartz cell. The rate of heating was set at 1 °C/min with hold steps of 10 min at each temperature. Values for the LCST of aqueous solutions of the polymers were determined at a temperature with a half of the optical transmittance between blow and above transitions. The critical micelle concentrations (CMC) of the copolymers were determined by fluorescence measurements using pyrene as a probe. A pyrene solution (in acetone) was added into a series of volumetric flasks in such an amount that the final concentration of pyrene in each solution was 6.0×10^{-7} mol/L; thereafter, the acetone was removed completely. The polymer solution was added into the volumetric flasks and diluted till the calibration mark using ultrapurified water to obtain the desired copolymer concentrations ranging from 1.0×10^{-4} to 0.9 mg/mL. The samples were stored at room temperature overnight to equilibrate the pyrene and micelles. Steady-state fluorescence excitation spectra were recorded on a Varian Cary Eclipse fluorescence spectrophotometer at 390-nm emission wavelength and 5.0-nm slit width. The scan rate was 120 nm/min. The size distribution of micelles was determined by dynamic light scattering (DLS) using a Malvern Nano ZS instrument. The morphology of the micelles was investigated by transmission electron microscopy (TEM), carried out on a Hitachi H-7650 electron microscope, operating at an accelerating voltage of 80 kV. Specimens were prepared by transferring a drop of the micelle solution onto a 200-mesh copper grid coated with carbon and allowing the sample to dry in air before measurements.

Results and discussion

Synthesis of poly(*N*-vinylcaprolactam)(PNVCL-OH)

The hydroxyl-terminated PNVCL-OH was synthesized by a radical polymerization of NVCL using 2-mercaptoethanol as a chain transfer agent and AIBN as an initiator (Scheme 1).

The IR spectrum of PNVCL-OH is depicted in Fig. 1B. The polymer gave a broad absorption in the 3,200–3,600 cm^{-1} region due to terminal hydroxyl groups. Furthermore, the absorption at 1,650 cm^{-1} was assigned to the stretch vibration $\nu_{C=O}$ from the PNVCL-OH segment; the typical absorption of the NVCL monomer at 1,630, 2,980 and 3,100 cm^{-1} had completely disappeared.

The ^1H NMR spectrum of PNVCL-OH was shown in Fig. 2A. The peak at 4.25–4.68 ppm is assigned to proton a in PNVCL segment. The peak at 3.75 ppm is assigned to protons i in the $–CH_2C\mathbf{H_2}OH$ segment. The peak at 2.95–3.42 ppm is assigned to protons c in PNVCL segment. The peak at 2.80 ppm is assigned to protons h in the $–C\mathbf{H_2}CH_2OH$ segment. The peak at 2.45–2.82 ppm is assigned to protons g in the PNVCL segment. The peak at 2.15 ppm is assigned to proton j in the $–CH_2CH_2O\mathbf{H}$ segment. The peaks at 1.00–2.06 ppm are assigned to protons b, d, e, f in the PNVCL segments.

The GPC trace of the PNVCL-OH is shown in Fig. 3A. The sample showed unimodal molecular weight distribution. This further indicates that the polymerization is completed successfully and there is no other compound in the reaction product.

Synthesis of poly(*N*-vinylcaprolactam)/poly(ε-caprolactone) (PNVCL-*b*-PCL) block copolymer

The amphiphilic block copolymers composed of PNVCL as the hydrophilic part and PCL as the hydrophobic one were synthesized through ring-opening polymerization. Stannous octoate, one of the most widely used initiators for cyclic esters polymerization, has been reported recently to induce polymerization of cyclic ε-caprolactone (ε-CL), lactide (LA), and phosphoester (PPE) by formation of stannous alcoholate active centers with ROH or RNH_2 as co-initiator [34–36]. Because PNVCL-OH contains hydroxyl group, it can initiate ring-opening polymerization of cyclic ε-CL to generate PNVCL-*b*-PCL block copolymers. A series of the block copolymers with various molecular weights were synthesized and the results are summarized in Table 1.

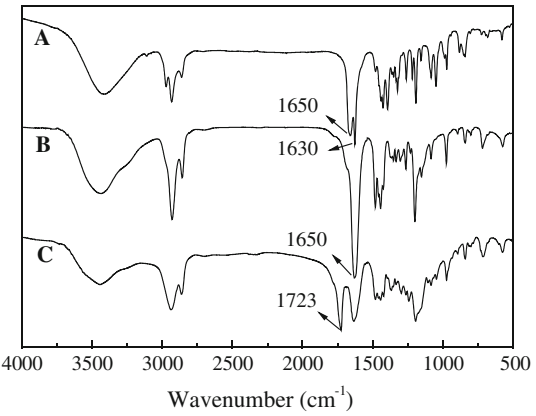

Fig. 1 IR spectra of NVCL (**A**), PNVCL-OH (**B**) and PNVCL-*b*-PCL**3** (**C**)

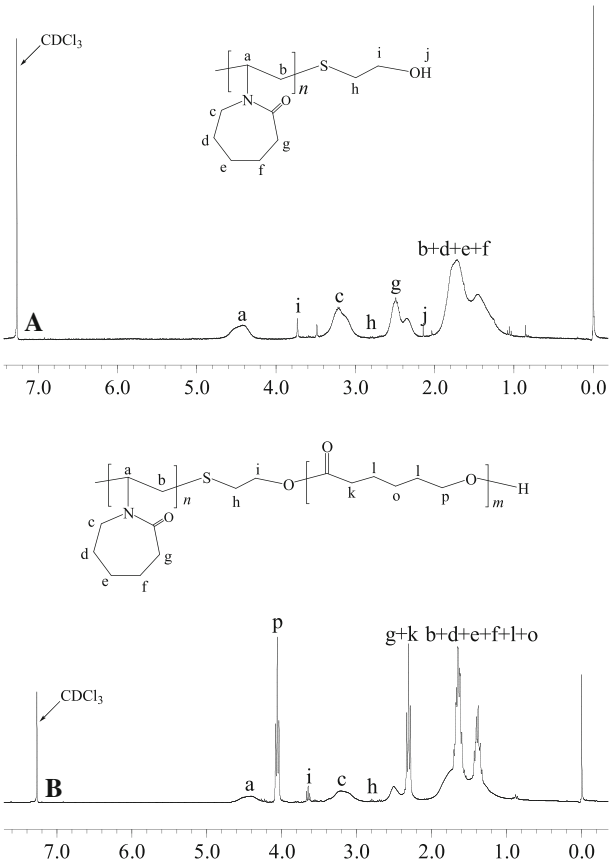

Fig. 2 ^{1}H NMR spectra of PNVCL-OH (**A**) and PNVCL-*b*-PCL**3** (**B**) block copolymer in $CDCl_3$

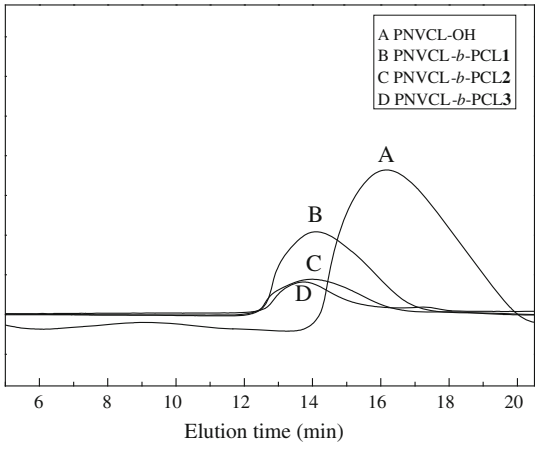

Fig. 3 GPC traces of PNVCL-OH and PNVCL-*b*-PCL block copolymers

The IR spectrum of PNVCL-*b*-PCL**3** was shown in Fig. 1C. Compared to PNVCL-OH (Fig. 1B), the spectrum of the copolymer clearly showed the most important vibration bands, especially the vibrations of $\nu_{C=O}$ appearing at 1,723 cm^{-1} from the PCL segment.

The ^1H NMR spectrum of PNVCL-*b*-PCL**3** block copolymer is shown in Fig. 2B. The peak at 4.25–4.68 ppm is assigned to proton a in PNVCL segment. The peak at 3.75 ppm is assigned to protons i in the $–CH_2C\mathbf{H_2}O–$ segment. The peak at 2.95–3.42 ppm is assigned to protons c in PNVCL segment. The peak at 2.80 ppm is assigned to protons h in the $–C\mathbf{H_2}CH_2O-$ segment. The peak at 4.11 ppm is assigned to protons *p* in the PCL segment. The peaks at 2.22–2.40 ppm are assigned to protons g, k in the PNVCL and PCL segments, respectively. The peaks at 1.32–1.78 ppm are assigned to protons *b*, *d*, *e*, *f*, *l*, *o* in the PNVCL and PCL segments, respectively. There are not additional peaks in the spectrum, which initially indicates that the block copolymer was prepared.

The GPC traces of the PNVCL-*b*-PCL copolymers were shown in Fig. 3. The three copolymers showed unimodal molecular weight distribution. This further indicates that the copolymerization is completed successfully and there is no homopolymer in the reaction product. GPC data of the copolymers are listed in Table 1.

Formation of micelles

The micellar structures of PNVCL-*b*-PCL are confirmed by fluorescence technique using pyrene as a probe. The fluorescence excitation spectra of pyrene in the presence of PNVCL-*b*-PCL**1** at various concentrations are shown in Fig. 4. A red shift from 333 to 337 nm is observed with increasing concentration of PNVCL-*b*-PCL**1**, indicating that micellization takes place for the PNVCL-*b*-PCL**1** copolymer. Such results can be attributed to the transfer of pyrene molecules from water to a hydrophobic environment within the micelles core.

The onset of micellization and the critical micelle concentrations (CMC) can also be obtained from the studies of excitation spectra [37]. For the copolymer PNVCL-*b*-PCL**1**, 333 and 337 nm are chosen as the peak wavelength of the (0, 0) band in the

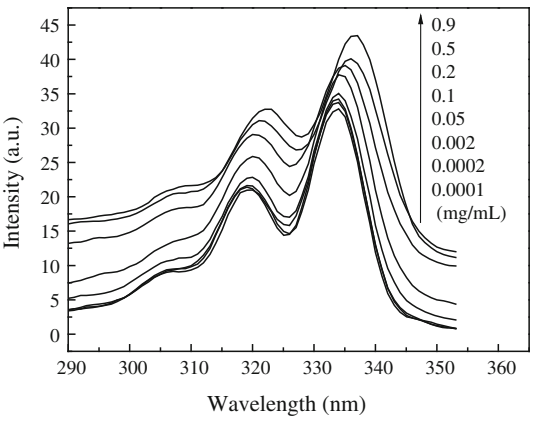

Fig. 4 Excitation spectra of pyrene as a function of PNVCL-*b*-PCL**1** concentration in water

pyrene excitation spectra in the aqueous phase and in the entirely hydrophobic core of polymeric micelle, respectively. The pyrene fluorescence intensity ratios (I_{337}/I_{333}) are plotted against the logarithm of copolymer concentration. The plots are shown in Fig. 5. Below a certain concentration, I_{337}/I_{333} is constant, above this concentration, I_{337}/I_{333} increases with increasing lg C and finally reaches a plateau. From this plot, the critical micelle concentration (CMC) of 2.7×10^{-2} mg mL^{-1} was obtained from the intersection of two straight lines: the base line and the rapidly rising I_{337}/I_{333} line. The CMC of PNVCL-*b*-PCL**2** and PNVCL-*b*-PCL**3** were also obtained from the same methods and listed in Table 1. The CMC values were reduced with the increasing of the proportion of PCL segment. It is reasonable since higher content of the hydrophobic segments will result in stronger interactions between hydrophobic chains, leading to a more stable structure and therefore to lower CMC value. This trend is in agreement with the reported result by the literature [38].

Size and size distribution of PNVCL-*b*-PCL micelles

The size and size distribution of micelles were measured by DLS. As shown in Fig. 6, the mean diameter of micelles formed by PNVCL-*b*-PCL**1**, PNVCL-*b*-PCL**2**, and PNVCL-*b*-PCL**3** were about 106, 142, and 167 nm, respectively. The size of micelle was increased with the increasing of the proportion of PCL segment, so the size of the copolymer micelle could be adjusted by changed the proportion of PCL segment of the copolymer. The increment of micelle size with increasing PCL block length is mainly originated from the increase of hydrophobic property by the longer hydrophobic PCL chain in aqueous milieu.

Thermosensitivity of polymers

Figure 7 is a typical photograph of aqueous solutions of PNVCL-*b*-PCL**2**. Below the LCST, PNVCL-*b*-PCL copolymers are amphiphilic, consisting of a hydrophilic block (PNVCL) and a hydrophobic block (PCL). The solution was transparent and colorless

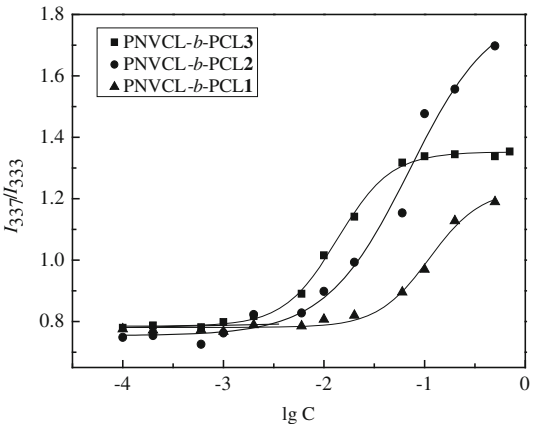

Fig. 5 Plots of I_{337}/I_{333} versus logarithm of PNVCL-*b*-PCL block copolymers' concentrations

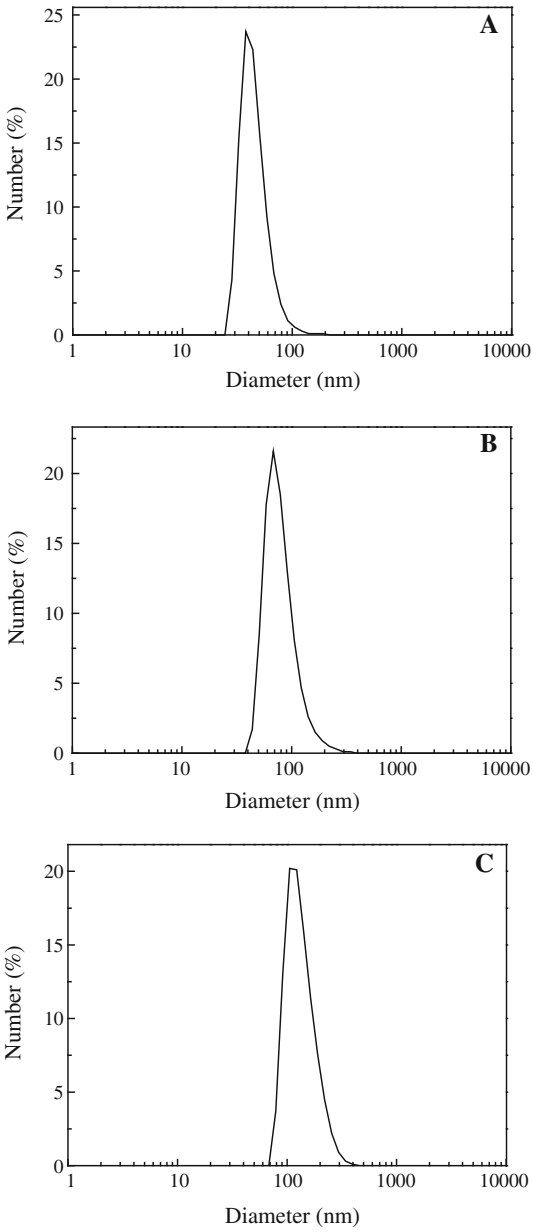

Fig. 6 The size distributions of PNVCL-*b*-PCL**1** (**A**), PNVCL-*b*-PCL**2** (**B**) and PNVCL-*b*-PCL**3** (**C**) block copolymer micelles in aqueous solution measured by DLS at 25 °C

(Fig. 7A). However, when heated closed to the LCST, the solution gradually turned into a semitransparent emulsion (Fig. 7B), then above the LCST, the copolymers are hydrophobic and the solution became a white opaque suspension (Fig. 7C), and finally the polymers precipitated from water if the solution was kept at a high temperature for enough time. When cooled, the semitransparent emulsion and transparent colorless solution were gotten again. Evidently, PNVCL-*b*-PCL**2** showed

Fig. 7 LCST transitions of PNVCL-*b*-PCL**2** at different temperatures: 25.6 °C (**A**), 38.9 °C (**B**) and 43.3 °C (**C**) ($c = 0.5$ mg/mL)

a revisable LCST phase transition in water. This phenomenon takes place due to the different solvation of poly(*N*-vinylcaprolactam) chains by water molecules at the temperatures below and above the phase transition temperature [39].

Effect of molecular weight on the LCST of PNVCL-OH

LCSTs are expected to decrease with increasing polymer molecular weight based on the changes in the polymer–solvent interaction [19, 40, 41]. This phenomenon is ascribed to the fact that the solution behavior of the PNVCL-OH/water system corresponds to a typical Flory-Huggins demixing behavior with LCST, also called Type I behavior [42]. Figure 8A shows a definite effect of the molecular weight on the LCST of PNVCL-OH in aqueous solution. The LCST decreased as the molecular weight of the polymer increased. The variation of the number-average molecular weight of PNVCL-OH from 2572 to 5383 g mol^{-1} leaded to the variation of the LCST from 47.8 to 38.6 °C (Fig. 8B). This result is explained by the fact that the decrease of the molecular weight leads to an increase of the polymer hydrophilicity. Moreover, the increase of the hydrophilicity would also be explained by the contribution of the hydroxyl end group from the chain transfer agent as was evidenced by Santos for PNVCL with molecular weights between 2.497×10^4 and 5.903×10^4 g/mol [43]. As the molecular weights obtained in this work were in general much lower than those obtained by Santos et al., the influence of the hydroxyl end group was more evident. Therefore, the increase of molecular weight seems to have a more effective influence on the LCST. The difference on the LCST values in the range of molecular weights studied observed in this work was much higher than that in the literature [41, 43].

Effect of hydrophobic block length on the LCST of copolymers

It is reported that the LCST of thermo-responsive polymers can be controlled by compositions of hydrophobic and hydrophilic units [18]. In this study, the LCST

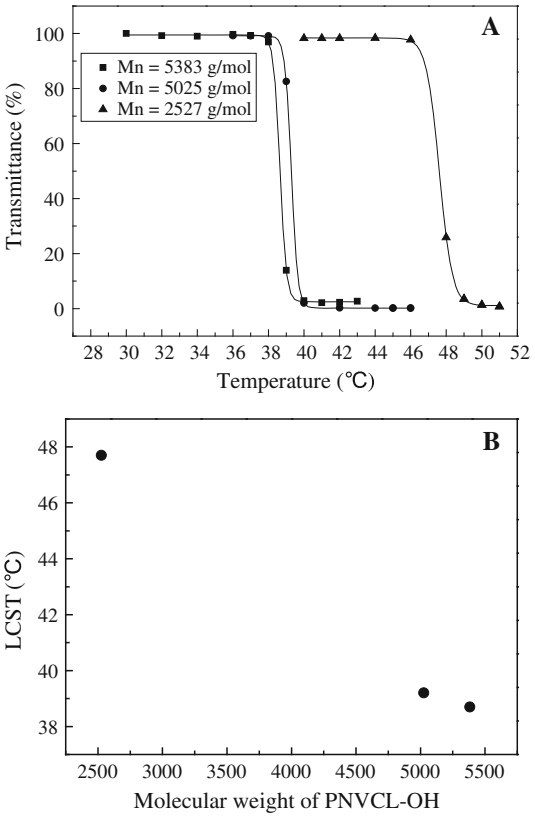

Fig. 8 Effects of molecular weight on the LCST of PNVCL-OH (**A**) and LCST as a function of the molecular weight (**B**) ($c = 5$ mg/mL)

transition behavior of the PNVCL-*b*-PCL block copolymers was tuned by changing the length of the hydrophobic PCL block: the larger the hydrophobic block content of the copolymer, the lower the LCST at fixed PNVCL molecular weight. Figure 9A shows the temperature dependence of optical transmittance of micellar solutions of the copolymers with different hydrophobic PCL block lengths. The transmittance decreased significantly at a specific temperature on heating solutions of all of the copolymers. The LCST were evaluated as 39.3, 37.5, 35.3, and 33.7 °C for PNVCL-OH, PNVCL-*b*-PCL**1**, PNVCL-*b*-PCL**2**, and PNVCL-*b*-PCL**3**, respectively (Fig. 9B), thus showing a decreasing trend with increasing PCL block length. The LCSTs of PNVCL-*b*-PCL polymers were found to be lower than PNVCL-OH homopolymers and to depend on their molecular weights. This is considered to result from hydrating contributions from polar terminal hydrophilic hydroxyl groups in the copolymers [44]. In general, the LCST decreases with decreasing hydrophilicity of the polymer. Considering the fact that PCL block is more hydrophobic than PNVCL block, it is reasonable that the LCST decreases with the increasing molar fraction of PCL.[15] These results clearly show that the phase transition of PNVCL-*b*-PCL can be controlled within a temperature range (33.7–39.3 °C) by varying the block length of the PCL block. Similar observations have been reported for several thermosensitive polymers [19, 45].

Thermoresponsivity under physiological conditions is effective for drug delivery or tissue engineering applications. In fact, the LCST of thermo-responsive polymers can be controlled by compositions of hydrophobic and hydrophilic units [14]. Thus, LCST can also be further tuned by adjusting the composition of the PNVCL block or adding new hydrophobic blocks to find its application under physiological temperatures.

Effect of concentration on the LCST of copolymers

Figure 10 shows the effect of concentration on the LCST of PNVCL-*b*-PCL**2** aqueous solution. For the lowest concentration (2.0×10^{-3} mg/mL, which was below the CMC), nearly 100 % transmittance was maintained in the tested

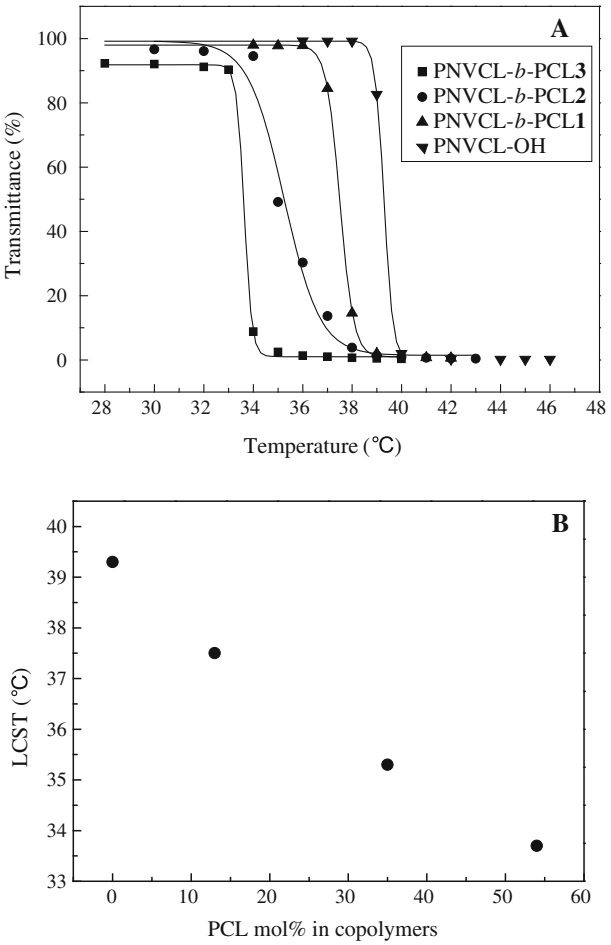

Fig. 9 Effect of hydrophobic block length on the LCST of copolymers (**A**) ($c = 5$ mg/mL) and LCST as a function of the PCL block in the copolymer (**B**)

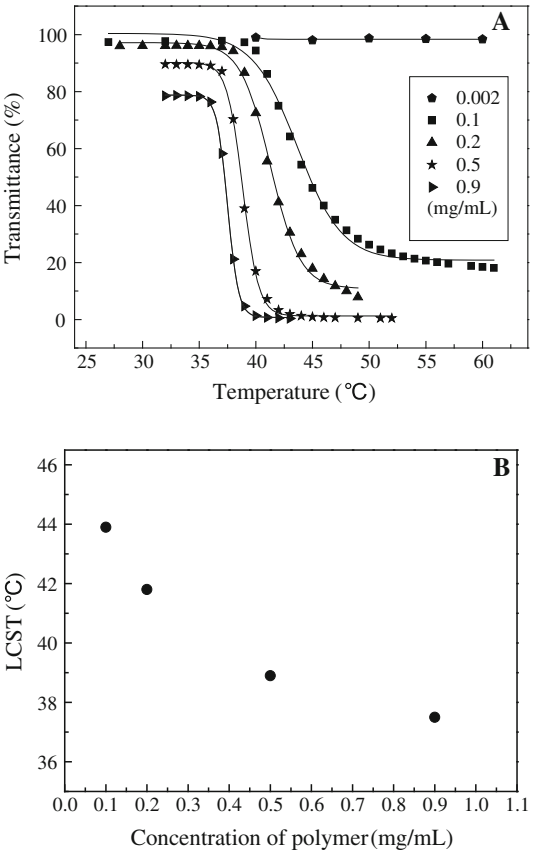

Fig. 10 Effect of concentration on the LCST of PNVCL-*b*-PCL**2** (**A**) and LCST as a function of the concentration of PNVCL-*b*-PCL**2** (**B**)

temperature range. As the polymer concentration became higher than the CMC and micelle formation occurred, the transmittance decreased sharply at about 43.9 °C on heating, indicating that a LCST transition readily occurred only in micellar solution. The polymer concentration had an effect on the LCST of the micellar solution: increasing the concentration from 0.1 to 0.9 mg/mL shifted the LCST 6.4 °C toward lower temperature. When the concentration is 0.9 mg/mL, LCST of the micellar solution was 37.5 °C. Similar observations have been reported for other thermo-sensitive polymers [46]. In addition, it should be noted that the sharpness of the thermally induced phase transition was dependent on the polymer concentration. A fairly sharp LCST transition was observed at concentrations of 0.9 and 0.5 mg/mL. At concentrations of 0.1 and 0.2 mg/mL, very limited variation of transmittance was displayed at the LCST. For concentrations >0.9 mg/mL, the transition became broader. This finding is consistent with the generally accepted LCST principle for dilute solutions, which states that higher water content enhances the hydrogen-bonding interactions between water and the polymer chain, which requires more thermal energy to break the water structure, thereby resulting in an increase of the LCST [21, 47].

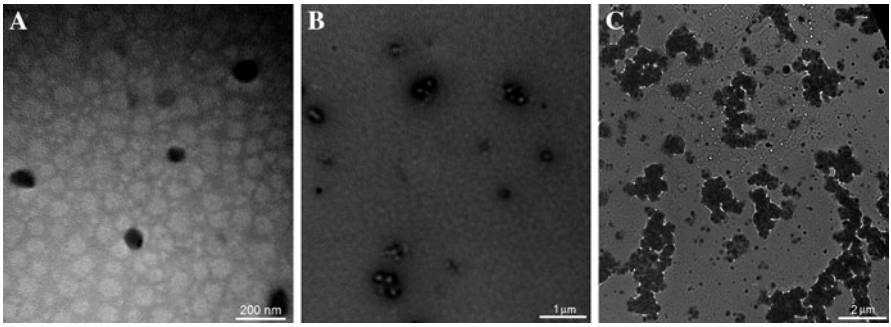

Fig. 11 TEM images of PNVCL-*b*-PCL**2** block copolymer micelles: (**A**) 25.6 °C, (**B**) 38.9 °C and (**C**) 43.3 °C (c = 0.5 mg/mL)

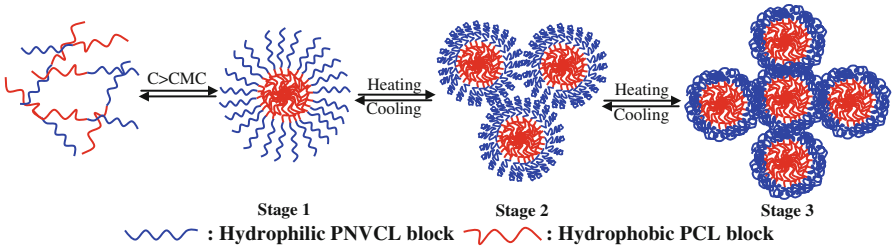

Scheme 2 Schematic illustration of thermally induced aggregation and phase transition of PNVCL-*b*-PCL copolymers in water

Variable temperature TEM measurements

Figure 11 shows TEM images of the micelles obtained by the self-assembly of PNVCL-*b*-PCL**2** block copolymer in aqueous solution at 25.6, 38.9, and 43.3 °C, respectively. All solution concentrations were kept at 0.5 mg/mL, which was above the CMC of PNVCL-*b*-PCL**2** solution. When the solution temperature was below the LCST [<38.9 °C, Scheme 2(Stage 1)], spherical polymer micelles existed individually (Fig. 11A) and the micellar solution was clear (Fig. 7A). At temperatures close to the LCST [Scheme 2(Stage 2)], intermicelle aggregation gave rise to formation of larger aggregates with multicore structure that was detectable in their TEM images (Fig. 11B) and associated with an abrupt increase in aggregate radius. Moreover, the solution became cloudy (Fig. 7B). When the temperature was 43.3 °C, the micelles aggregated [Fig. 11C, Scheme 2(Stage 3)]. The micelle dehydration and aggregation will certainly increase the solution turbidity due to the scattering (Fig. 7C).

Conclusions

In the present study, the PNVCL-OH and PNVCL-*b*-PCL block copolymers with different PCL block lengths have been synthesized. The structures and compositions

of the polymers characterized by FT-IR, ^{1}H NMR and GPC. The nanosized micelles with a core–shell (corona) structure and regularly spherical shape were obtained by self-assembly from the block copolymer in aqueous solution. The property of micelles such as CMC and size was investigated. It has been revealed that the phase transition of PNVCL-*b*-PCL micelles is reversible. The LCST of PNVCL-OH is affected by the molecular weight. The LCST of PNVCL-*b*-PCL is affected by the composition and the concentration of the copolymer, which allows convenient adjustment of their thermosensitivity.

Acknowledgments The authors are grateful to the financial supports from the Natural Science Foundation for Education Department of Liaoning Province of China (No. L2012007), Program for Liaoning Innovative Research Team in University (No. LT2011001) and Foundation of 211 Project for Innovative Talents Training, Liaoning University.

References

1. Kuramochi H, Andoh Y, Yoshii N, Okazaki S (2009) All-atom molecular dynamics study of a spherical micelle composed of *N*-acetylated poly(ethylene glycol)-poly(γ-benzyl L-glutamate) block copolymers: a potential carrier of drug delivery systems for cancer. J Phys Chem B 113:15181–15188
2. Zhang JX, Ellsworth K, Ma PX (2010) Hydrophobic pharmaceuticals mediated self-assembly of β-cyclodextrin containing hydrophilic copolymers: novel chemical responsive nano-vehicles for drug delivery. J Controlled Release 145:116–123
3. Cai CH, Lin JP, Chen T, Tian XH (2010) Aggregation behavior of graft copolymer with rigid backbone. Langmuir 26:2791–2797
4. Peng CL, Shieh MJ, Tsai MH, Chang CC, Lai PS (2008) Self-assembled star-shaped chlorin-core poly(ε-caprolactone)-poly(ethylene glycol) diblock copolymer micelles for dual chemo-photodynamic therapies. Biomaterials 29:3599–3608
5. Zhang XW, Oddon M, Giani O, Monge S, Robin JJ (2010) Novel strategy for ROP of NCAs using thiols as initiators: synthesis of diblock copolymers based on polypeptides. Macromolecules 43:2654–2656
6. Hu Y, Jiang ZP, Chen R, Wu W, Jiang XQ (2010) Degradation and degradation-induced re-assembly of PVP-PCL micelle. Biomacromolecules 11:481–488
7. Yao J, Ruan YL, Zhai T, Guan J, Tang GP, Li HR, Dai S (2011) ABC block copolymer as "smart" pH-responsive carrier for intracellular delivery of hydrophobic drugs. Polymer 52:3396–3404
8. Li YY, Zhang XZ, Cheng H, Zhu JL, Cheng SX, Zhuo RX (2006) Self-assembled, thermosensitive PCL-*g*-P(NIPAAm-*co*-HEMA) micelles for drug delivery. Macromol Rapid Commun 27:1913–1919
9. Virtanen J, Tenhu H (2001) Studies on copolymerization of *n*-isopropylacrylamide and glycidyl methacrylate. J Polym Sci Part A Polym Chem 39:3716–3725
10. Wang YC, Tang LY, Li Y, Wang J (2009) Thermoresponsive block copolymers of poly(ethylene glycol) and polyphosphoester: thermo-induced self-assembly, biocompatibility, and hydrolytic degradation. Biomacromolecules 10:66–73
11. Bigot J, Charleux B, Cooke G, Delattre F, Fournier D, Lyskawa J, Sambe L, Stoffelbach F, Woisel P (2010) Tetrathiafulvalene end-functionalized poly(*N*-isopropylacrylamide): a new class of amphiphilic polymer for the creation of multistimuli responsive micelles. J Am Chem Soc 132:10796–10801
12. Kumar A, Srivastava A, Galaev IY, Mattiasson B (2007) Smart polymers: physical forms and bioengineering applications. Prog Polym Sci 32:1205–1237
13. Qu TH, Wang AR, Yuan JF, Shi JH, Gao QY (2009) Preparation and characterization of thermoresponsive amphiphilic triblock copolymer and its self-assembled micelle for controlled drug release. Colloids Surf B Biointerfaces 72:94–100
14. Iwasaki Y, Wachiralarpphaithoon C, Akiyoshi K (2007) Novel thermoresponsive polymers having biodegradable phosphoester backboness. Macromolecules 40:8136–8138

15. Liu X, Ni PH, He JL, Zhang MZ (2010) Synthesis and micellization of pH/temperature-responsive double-hydrophilic diblock copolymers polyphosphoester-*block*-poly[2-(dimethylamino)ethyl methacrylate] prepared via ROP and ATRP. Macromolecules 43:4771–4781
16. Vihola H, Laukkanen A, Tenhu H, Hirvonen J (2008) Drug release characteristics of physically cross-linked thermosensitive poly(*N*-vinylcaprolactam) hydrogel particles. J Pharm Sci 97:4783–4793
17. Prabaharan SM, Grailer JJ, Steeber DA, Gong SQ (2008) Stimuli-responsive chitosan-*graft*-poly(*N*-vinylcaprolactam) as a promising material for controlled hydrophobic drug delivery. Macromol Biosci 8:843–851
18. Shah S, Pal A, Gude R, Devi S (2010) Synthesis and characterization of thermo-responsive copolymeric nanoparticles of poly(methyl methacrylate-*co*-*N*-vinylcaprolactam). Eur Polym J 46:958–967
19. Viholal H, Laukkanen A, Valtola L, Tenhu H, Hirvonen J (2005) Cytotoxicity of thermosensitive polymers poly(*N*-isopropylacrylamide), poly(*N*-vinylcaprolactam) and amphiphilically modified poly(*N*-vinylcaprolactam). Biomaterials 26:3055–3064
20. Loos W, Verbrugghe S, Goethals EJ, Prez FED, Bakeeva IV, Zubov VP (2003) Thermo-responsive organic/inorganic hybrid hydrogels based on poly(*N*-vinylcaprolactam). Macromol Chem Phys 204:98–103
21. Verbrugghe S, Bernaerts K, Prez FED (2003) Thermo-responsive and emulsifying properties of poly(*N*-vinylcaprolactam) based graft copolymers. Macromol Chem Phys 204:1217–1225
22. Hurtgen M, Liu J, Debuigne A, Jerome C, Detrembleur C (2012) Synthesis of thermo-responsive poly(*N*-vinylcaprolactam)-containing block copolymers by cobalt-mediated radical polymerization. J Polym Sci Part A Polym Chem 50:400–408
23. Lequieu W, Shtanko NI, Prez FED (2005) Track etched membranes with thermo-adjustable porosity and separation properties by surface immobilization of poly(*N*-vinylcaprolactam). J Membr Sci 256:64–71
24. Dimitrov I, Trzebicka B, Müller AHH, Dworak A, Tsvetanov CB (2007) Thermosensitive water-soluble copolymers with doubly responsive reversibly interacting entities. Prog Polym Sci 32:1275–1343
25. Castillo RV, Müller AJ, Raquez JM, Dubois P (2010) Crystallization kinetics and morphology of biodegradable double crystalline PLLA-*b*-PCL diblock copolymers. Macromolecules 43:4149–4160
26. Loh XJ, Sng KBC, Li J (2008) Synthesis and water-swelling of thermo-responsive poly(ester urethane)s containing poly(ε-caprolactone), poly(ethylene glycol) and poly(propylene glycol). Biomaterials 29:3185–3194
27. Li JB, Ren J, Cao Y, Yuan WZ (2010) Synthesis of biodegradable pentaarmed star-block copolymers via an asymmetric BIS-TRIS core by combination of ROP and RAFT: from star architectures to double responsive micelles. Polymer 51:1301–1310
28. Rong GZ, Deng MX, Deng C, Tang ZH, Piao LH, Chen XS, JingX B (2003) Synthesis of poly(ε-caprolactone)-*b*-poly(γ-benzyl-L-glutamic acid) block copolymer using amino organic calcium catalyst. Biomacromolecules 4:1800–1804
29. Sahoo S, Sasmal A, Nanda R, Phani AR, Nayak PL (2010) Synthesis of chitosan-polycaprolactone blend for control delivery of ofloxacin drug. Carbohydr Polym 79:106–113
30. Sarazin P, Li G, Orts WJ, Favis BD (2008) Binary and ternary blends of polylactide, polycaprolactone and thermoplastic starch. Polymer 49:599–609
31. Loontjens CAM, Vermonden T, Leemhuis M, Van Steenbergen MJ, Van Nostrum CF, Hennink WE (2007) Synthesis and characterization of random and triblock copolymers of ε-caprolactone and (benzylated) hydroxymethyl glycolide. Macromolecules 40:7208–7216
32. Miguel VS, Limer AJ, Haddleton DM, Catalina F, Peinado C (2008) Biodegradable and thermoresponsive micelles of triblock copolymers based on 2-(*N*,*N*-dimethylamino)ethyl methacrylate and ε-caprolactone for controlled drug delivery. Eur Polym J 44:3853–3863
33. Zhang GL, Liang F, Song XM, Liu DL, Li MJ, Wu QH (2010) New amphiphilic biodegradable β-cyclodextrin/poly(L-leucine) copolymers: synthesis, characterization, and micellization. Carbohydr Polym 80:885–890
34. Xiao CS, Wang YC, Du JZ, Chen XS, Wang J (2006) Kinetics and mechanism of 2-ethoxy-2-oxo-1,3,2-dioxaphospholane polymerization initiated by stannous octoate. Macromolecules 39:6825–6831
35. Kowalski A, Duda A, Penczek S (2000) Kinetics and mechanism of cyclic esters polymerization initiated with tin(II) octoate. 3. Polymerization of L,L,-dilactide. Macromolecules 33:7359–7370

36. Kowalski A, Libiszowski J, Biela T, Cypryk M, Duda A, Penczek S (2005) Kinetics and mechanism of cyclic esters polymerization initiated with tin(II) octoate. polymerization of ε-caprolactone and L,L,-lactide co-initiated with primary amines. Macromolecules 38:8170–8176
37. Deng C, Chen XS, Yu HJ, Sun J, Lu TC, Jing XB (2007) A biodegradable triblock copolymer poly(ethylene glycol)-*b*-poly(L,-lactide co-initiated with primary amines-lactide)-*b*-poly(L-lysine): synthesis, self-assembly, and RGD peptide modification. Polymer 48:139–149
38. Wu QH, Wang C, Zhang D, Song XM, Wang LP, Zhang GL (2012) Synthesis and micellization of a new amphiphilic star-shaped poly(D, L,-lactide co-initiated with primary amines-lactide)/polyphosphoester block copolymer. React Funct Polym 72:372–377
39. Hain J, Schrinner M, Lu Y, Pich A (2008) Design of multicomponent microgels by selective deposition of nanomaterials. Small 4:2016–2024
40. Meeussen F, Nies E, Berghmans H, Verbrugghe S, Goethals E, Du Prez F (2000) Phase behaviour of poly(*N*-vinyl caprolactam) in water. Polymer 41:8597–8602
41. Laukkanen A, Valtola L, Winnik FM, Tenhu H (2004) Formation of colloidally stable phase separated poly(*N*-vinylcaprolactam) in water: a study by dynamic light scattering, microcalorimetry, and pressure perturbation calorimetry. Macromolecules 37:2268–2274
42. Shtanko NI, Lequieu W, Goethals EJ, Du Prez FE (2003) pH- and thermo-responsive properties of poly(*N*-vinylcaprolactam-*co*-acrylic acid) copolymers. Polym Int 52:1605–1610
43. Medeiros SF, Barboza JCS, Ré MI, Giudici R, Santos AM (2010) Solution polymerization of *N*-vinylcaprolactam in 1,4-dioxane. Kinetic dependence on temperature, monomer, and initiator concentrations. J Appl Polym Sci 118:229–240
44. Kohori F, Sakai K, Aoyagi T, Yokoyama M, Sakurai Y, Okano T (1998) Preparation and characterization of thermally responsive block copolymer micelles comprising poly(*N*-isopropylacrylamide-*b*-DL-lactide). J Controlled Release 55:87–98
45. Maeda Y, Tsubota M, Ikeda I (2003) Temperature-responsive graft copolymers with poly(propylene glycol) side chains. Macromol Rapid Commun 24:242–245
46. Kim YS, Gil ES, Lowe TL (2006) Synthesis and characterization of thermoresponsive-*co*-biodegradable linear-dendritic copolymers. Macromolecules 39:7805–7811
47. Shao LD, Hu MQ, Chen L, Xu L, Bi YM (2012) RAFT polymerization of *N*-vinylcaprolactam and effects of the end group on the thermal response of poly(*N*-vinylcaprolactam). React Funct Polym 72:407–413